Vol. B19 (1988) ACTA PHYSICA POLONICA No 3

APPLICATION OF FLUCTUATION ANALYSIS AND STATISTICAL TESTS FOR THE $^{12}C + ^{16}O$ REACTIONS IN THE ENERGY RANGE E_{cm} = 12.4–13.9 MeV

BY J. SZMIDER AND S. WIKTOR

Institute of Nuclear Physics, Cracow*

(*Received December 29, 1986; revised version received October 2, 1987*)

The excitation functions for various exit channels of $^{12}C + ^{16}O$ reactions, leading to different final states of ^{24}Mg, ^{26}Al and ^{27}Al, were measured in 53.6 keV steps over the incoming energy interval of ^{16}O ions from 12.4 to 13.9 MeV in the c.m. system. All measurements were performed at fixed lab. angle of 30°. Subsequent fluctuation analysis concerned excitation functions for several states of each final nucleus with excitations ranging up to 10 MeV and 4 MeV in ^{24}Mg and ^{26}Al, respectively, and from 6.4 to 11.4 MeV in ^{27}Al. Statistical tests applied to these excitation functions have revealed pronounced non statistical structures at the incident energies of 12.57, 12.73, 13.11 and 13.41 MeV in c.m. system.

PACS numbers: 25.70.-z

1. Introduction

The compound nucleus model has been successfully used [1–5] to explain the main features of reactions induced by heavy ions. The standard [6] statistical theory accounts fairly well for the magnitude of the energy averaged cross-sections, while rapid fluctuations are explained by Ericson's theory [7, 8]. In particular, the compound system of ^{28}Si nucleus, formed in the $^{12}C + ^{16}O$ reaction, has been extensively investigated by the application of fluctuation analysis in a wide range of excitation energies with the aim of establishing a dominant reaction mechanism and extracting some compound nucleus parameters. Halbert et al. [2], while analyzing the $^{12}C(^{16}O, \alpha)^{24}Mg$ reaction leading to low lying states of ^{24}Mg, have concluded that the results of the analysis are compatible with the simplified statistical theory. Selective populations of high spin states in ^{24}Mg were explained by Greenwood et al. [9] in terms of the compound nucleus reaction mechanism as a result of the formation and decay of high spin states of ^{28}Si. Kolata et al. [10] could not exclude the possibility that the statistical model is able to predict the average cross-sections, although in the interval of higher excitations several anomalies in the excitation functions were found.

* Address: Instytut Fizyki Jądrowej, Radzikowskiego 152, 31-342 Kraków, Poland.

Despite this success of the statistical model, detailed studies [11–19] of the $^{12}C + ^{16}O$ system have revealed that at both low, and high excitations many reactions proceed through resonances. In the compound ^{28}Si nucleus several resonances and resonancelike structures were found at excitation energies ranging from 20 up to 37 MeV. Thus, studying the $^{12}C + ^{16}O$ system, one observes both the fluctuations and correlated structures with the widths ranging from 70 keV to 2 MeV.

The present paper reports the results of the measurements and of the fluctuation analysis of the cross-sections for many exit channels corresponding to $^{27}Al + p$, $^{26}Al + d$ and $^{24}Mg + \alpha$ final states originated in the $^{12}C + ^{16}O$ reaction. The measurements were performed over the c.m. energy range from 12.4 to 13.9 MeV at $\theta_{lab} = 30°$. The procedures of the fluctuation analysis are summarized.

2. *Experimental method and results*

A beam of ^{16}O ions from the Université de Montreal EN Tandem Accelerator was used to bombard the target made of selfsupporting carbon foil 10 μg/cm² thick. Charged reaction products from the $^{12}C + ^{16}O$ reaction were detected by the telescope placed at $\theta_{lab} = 30°$. The telescope consisted of the 166 μ ΔE and 2000 μ E-detectors.

Due to the lack of a thicker E-detector the excitation functions for the $^{27}Al + p$ exit channels were measured only for excitations of the ^{27}Al final nucleus higher than 6.4 MeV. The carbon buildup on the target was estimated from the comparison of counting rates for a given reaction obtained at some reference beam energy (practically at the energy of the first run when carbon deposit was assumed to be zero).

The excitation functions, several of which are shown in Fig. 1, were measured in the c.m. energy interval ranging from 12.4 to 13.9 MeV in 53.6 keV steps. Errors of relative yields were mainly due to carbon builtup correction, counting statistic and background subtraction. In most cases they were estimated to be smaller than 5%.

The γ-ray yields for several exit channels in the $^{12}C + ^{16}O$ system such as $^{24}Mg + \alpha$, $^{23}Na + \alpha p$, $^{20}Ne + 2\alpha$, and $^{26}Al + np$, used in the frequency distribution analysis and in the binomial test for nonstatistical structures, have been taken from another experiment [14].

3. *Fluctuation analysis*

The fluctuation analysis provides a tool for establishing whether the dominant reaction mechanism is consistent with the compound nucleus model when the conditions inherent in the statistical model are fulfilled. The results of the analysis enable one to determine the average properties of the compound system — such as the coherence width Γ_c of fluctuating component of cross-section, the contribution of the direct part of the cross-section to the total cross-section Y_d, and the number of effective channels N_{eff}. Straightforward results of the fluctuation analysis are influenced by the reaction process and by the experimental conditions.

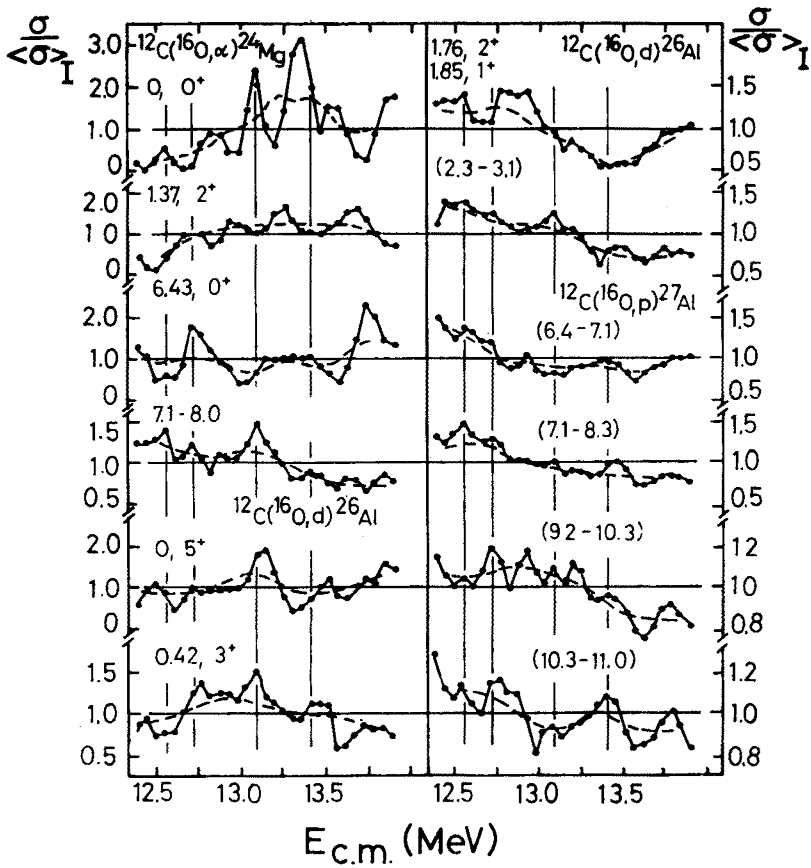

Fig. 1. Examples of excitation functions for transitions to the selected single states and uresolved groups of states in ^{24}Mg, ^{26}Al and ^{27}Al. The dashed curves represent the running average with $\Delta = 375$ keV

First we consider the influence of the reaction process on the parameters determined from analysis. Usually the measured excitation function consists of fluctuations imposed upon a slowly varying broader structure, which from now on will be called a "trend". The procedures of fluctuation analysis require the trend to be removed. In order to do this the data were reduced by a method of running averages

$$x(E_i) = \frac{\sigma(E_i)}{\langle\sigma(E)\rangle_\Delta}, \tag{1}$$

where $\sigma(E_i)$ is the differential cross-section at an energy E and $\langle\sigma(E)\rangle_\Delta$ is the cross-section averaged over a subinterval Δ i.e.

$$\langle\sigma(E)\rangle_\Delta = \frac{1}{P}\sum_{E_i-\frac{1}{2}\Delta}^{E_i+\frac{1}{2}\Delta}\sigma(E_i),$$

where P is the number of points in the interval Δ. The dashed lines of Fig. 1 show the running averages of the data, taken over the interval of $\Delta = 375$ keV. The autocorrelation function for the trend free data can be written as:

$$C_r(\varepsilon) = \left\langle \left[\frac{\sigma(E)}{\langle \sigma(E) \rangle_\Delta} - 1 \right] \left[\frac{\sigma(E+\varepsilon)}{\langle \sigma(E+\varepsilon) \rangle_\Delta} - 1 \right] \right\rangle \tag{2}$$

where ε is the energy increment.

For small values of ε, i.e. for $\varepsilon \ll I$, where I is the total energy interval under consideration, the following relations has been derived [21]:

$$C(\varepsilon) = C(0) \frac{\Gamma_c^2}{\Gamma_c^2 + \varepsilon^2}, \tag{3}$$

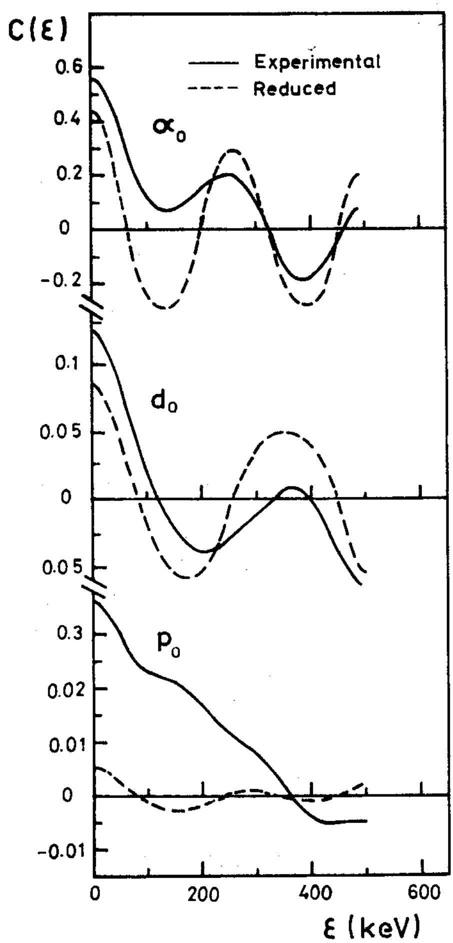

Fig. 2. The auto-correlation functions calculated with $\varepsilon = 53.6$ keV steps. The full curves correspond to non reduced data, the dashed curves correspond to the reduced data i.e. these after removing the trend by running average technique with $\Delta = 375$ keV

with

$$C(0) = \frac{(1-Y_d^2)}{N_{eff}}, \tag{4}$$

where Γ_c is the coherence width for a purely statistical process. The fluctuation parameters N_{eff} and Y_d are the effective number of open channels and the ratio of the direct part of the cross-section to the total cross-section, respectively. The procedure of running averages causes some reduction [8, 22, 23] of the coherence width Γ_c, which is visible also in Fig. 2, where some examples of autocorrelation functions are presented. Strong oscillations and large disagreement between the proton channel curves are evidently due to the finite sample size. The reduced values of Γ_c will further be denoted by Γ_r.

The problem of relations between the fluctuation parameters extracted from finite range data and their true values, determined from infinite sample size, was investigated by several authors [22, 24]. In the following analysis the Roeders [25] results were adopted. All the parameters, obtained with the use of reduced excitation functions, were corrected according to the procedures described in the appendices A and B.

4. *Distribution of cross-sections*

For the general case ($N_{eff} \geqslant 1$, $Y_d \geqslant 0$) the statistical model predicts a distribution of cross-sections in the form [22]:

$$P_{Ny}(x) = \left(\frac{N}{1-y}\right)^N x^{N-1} e^{-\frac{N(x+y)}{(1-y)}} \frac{I_{N-1}(2iz)}{(iz)^{N-1}}, \tag{5}$$

where $z = N\sqrt{xY_d}/(1-Y_d)$, $I_{N-1}(z)$ is a cylindrical Bessel's function of the imaginary argument $y = Y_d$ and $x = \frac{\sigma}{\langle\sigma\rangle}$. In order to find the parameters N and Y_d, the frequency distributions given by Eq. (5) were fitted to the experimental distributions of x by minimizing χ^2, defined as follows:

$$\chi^2 = \sum_i [P_{\Delta x}(x_i) - \int_{x_i-\frac{1}{2}\Delta x}^{x_i+\frac{1}{2}\Delta x} P_{Ny}(x)dx]^2 [\int_{x_i-\frac{1}{2}\Delta x}^{x_i+\frac{1}{2}\Delta x} P_{Ny}(x)dx]^{-1}, \tag{6}$$

where $P_{\Delta x}(x_i)$ is the experimental probability of finding x_i within the interval of Δx. From the best fit of χ^2 the N_r and Y_r parameters were deduced and corrected for the finite range effects, as shown in appendices A and B.

The lengths of the energy span Δ, used in the procedure of running averages, varied from 0.22 to 0.86 MeV. As demonstrated in Fig. 3 there exists for all channels a set of Δ-values for which $C(0)$ are independent of Δ. The derivatives $\Delta C_r(0)/C_r(0)$, presented on the left side of this figure, exhibit minima for the value of $\Delta_{cm} \approx 375$ keV. Further analyses in terms of the running average method were carried out with the use of this energy span.

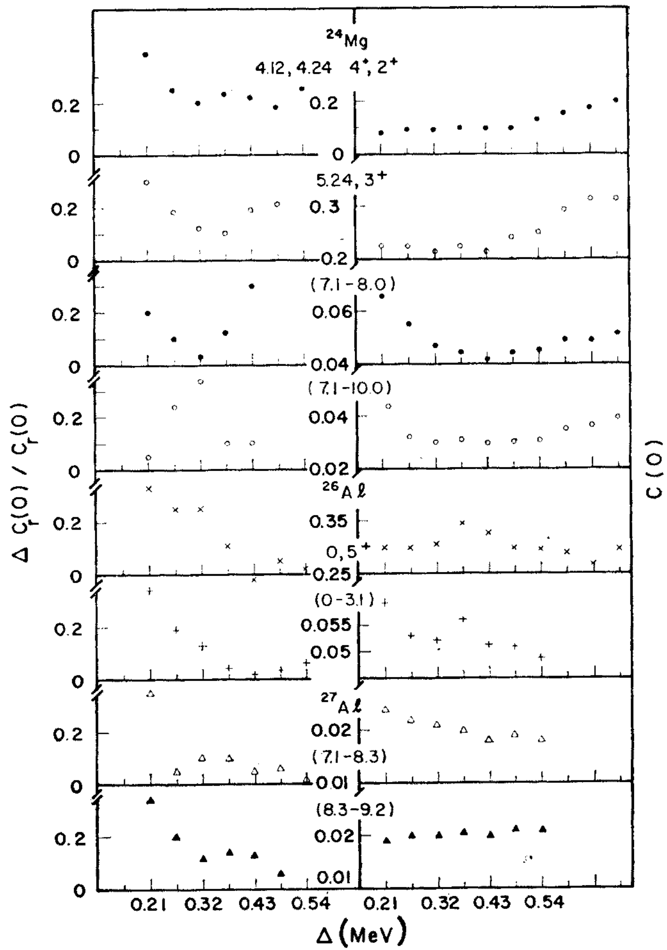

Fig. 3

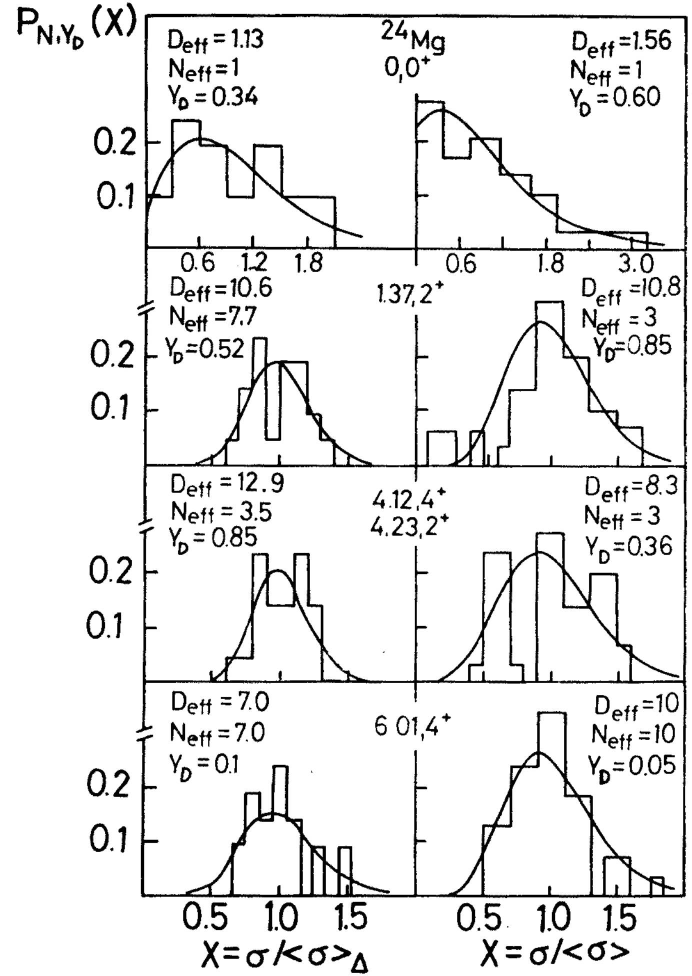

Fig. 4

Fig. 3. Dependence of derivative $\Delta C_r(0)/C_r(0)$ and $C(0)$ on the width of the averaging interval Δ

Fig. 4. Histograms and the statistical frequency distributions for transitions to the single states and to the doublet of states of ^{24}Mg. On the left hand

TABLE I

Parameters determined from frequency distribution

E_x (MeV) J^π	N_{eff}		Y_d		D_{eff}		σ_x
	a	*b*	*a*	*b*	*a*	*b*	
^{24}Mg							
0 0^+	1	1	0.60	0.34	1.56	1.13	
1.37 2^+	3	7.7	0.85	0.52	10.8	10.6	
4.1, 4.2 $4^+, 2^+$	3	3.5	0.36	0.854	8.3	12.9	
5.24 3^+	7	1.4	0.05	0.78	7.0	3.6	
6.01 4^+	10	7.0	0.05	0.09	10.0	7.0	
6.43 0^+	3	2.1	0.09	0.70	3.0	4.1	
0 - 6.43	5	1.4	0.90	0.93	26.3	10.2	
7.1- 8.0	10	7.7	0.80	0.85	27.8	28.4	
8.0- 8.4	2	3.5	0.90	0.78	10.5	8.9	
7.1-10.0	10	8.4	0.85	0.85	36.0	31.0	
^{26}Al							
0 5^+	7	3.5	0.05	0.30	7.0	3.8	
0.42 3^+	4	5.6	0.85	0.78	14.4	14.2	
1.06 1^+	6	2.8	0.20	0.70	6.3	5.5	
1.76, 1.8 $2^+, 1^+$	3	7.7	0.80	0.85	8.3	28.5	
2.07 4^+	5	7.7	0.75	0.85	11.4	28.5	
2.3-3.1	12	—	0.55	—	17.2	—	0.09
3.1-3.9	10	7.7	0.20	0.854	10.4	28.5	
3.9-4.0	10	4.9	0.10	0.70	10.0	9.6	
0.0-4.0	11	—	0.90	—	58	—	0.1
^{27}Al							
6.4- 7.1	12	—	0.65	—	20.8	—	0.08
7.1- 8.3	11	—	0.70	—	21.6	—	0.08
8.3- 9.2	10	—	0.85	—	36	—	0.08
9.2-10.3	10	—	0.90	—	53	—	0.06
10.3-11.0	11	—	0.90	—	58	—	0.09
11.0-11.4	9	—	0.90	—	47	—	0.08

a — results of analysis using the experimental excitation functions, *b* — results of analysis using the trend free excitation functions.

The experimental and calculated distributions of cross-sections are shown in Figs 4 and 5. If one defines a damping factor of the distribution as

$$D_{eff} = \frac{N_{eff}}{1 - Y_d^2}$$

the parameters N_{eff} and Y_d can be used to evaluate it. The autocorrelation coefficients $C(0)$, according to formula (4) are given by $C(0) = D_{eff}^{-1}$. The parameters determined from the frequency distributions are given in Table I. For some cases ($Y_d \approx 1$) instead

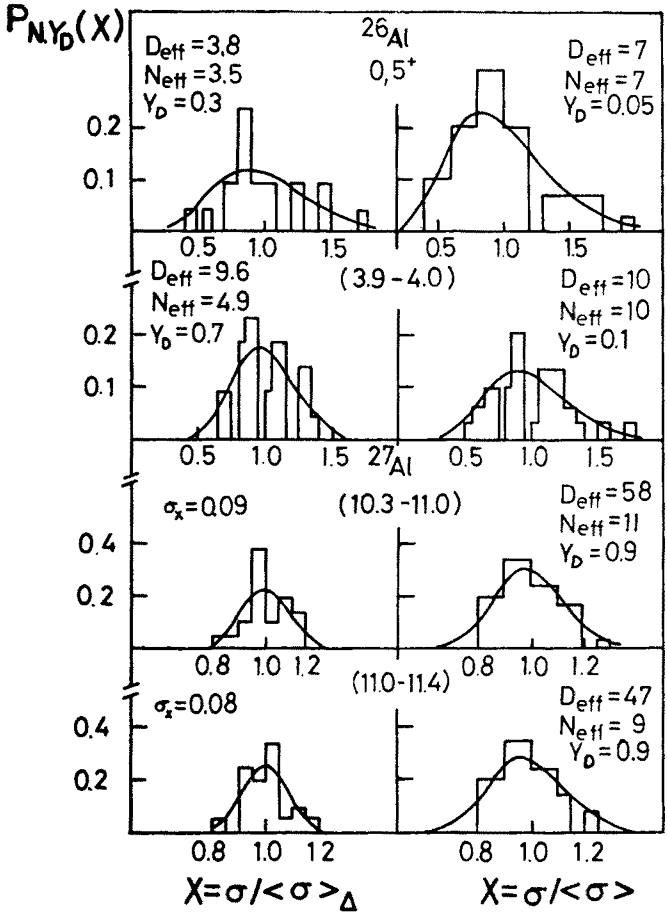

Fig. 5. The same as in Fig. 4 for a single state and for the group of states of ^{26}Al and ^{27}Al

of formula (5), the cross-section distributions were fitted by gaussian formula. The standard deviations σ_x, obtained from the fitting procedure, are given in Fig. 5 as well as in the last column of Table I. The inaccuracy of formula (5) discussed in the paper of Witala et al. [26] has also been considered. However, in our case that inaccuracy cannot change the picture substantially.

5. Parameters determined from autocorrelation

The fluctuation analysis has been carried out for both the experimental and the reduced (trend free) excitation functions. Numerical values of the parameters D_{eff} and Γ_a are given in Table II. The parameters extracted from the experimental (non reduced) excitation functions are listed in subcolumns *a* and the same parameters deduced from the reduced data by application of the averaging procedure, are listed in subcolumns *b*. The influence

TABLE II

Parameters determined from autocorrelations

E_x (MeV) J^π		D_{eff} *a*	D_{eff} *b*	$N_{\mathrm{eff}}^{\mathrm{H.F.}}$	Y_{d}	Γ_a (keV) *a*	Γ_a (keV) *b*	Γ_M (keV)
^{24}Mg								
0	0^+	1.1±0.5	1.0±0.5	1	0.25±0.30	93	100	104±3
1.37	2^+	6.0±2.1	9.4±3.9	3	0.84±0.09	122	130	114±17
4.1, 4.2	$4^+, 2^+$	7.0±2.4	12.0±5.0	7	0.66±0.25	203	79	124±11
5.24	3^+	2.9±1.1	5.0±2.2	3	0.55±0.30	165	103	84±4
6.01	4^+	10.2±3.5	7.1±3.0	4	0.66±0.30	117	124	105±6
6.43	0^+	3.6±1.3	2.6±1.2	1	0.84±0.08	80	133	114±30
0 -6.43		20.4±6.8	11.0±4.6	18	0.0	133	68	86±17
7.1- 8.0		18.6±6.2	24.0±9.7	13^c	0.70±0.25	138	96	114±4
8.0- 8.4		10.0±3.4	6.8±2.9	9^c	0.0 ±0.51	104	103	133±17
7.1-10.0		40.0±14	33.0±13	56	0.0	83	91	73±2
^{26}Al								
0	5^+	7.8±2.8	3.6±1.6	13^c	0.0	85	135	108±10
0.42	3^+	15.0±5.2	15.0±6	9^c	0.62±0.30	—	145	105±7
1.06	1^+	7.7±2.7	8.3±3.5	3^c	0.75±0.12	—	126	127±28
1.6, 1.8	$2^+, 1^+$	11.0±3.7	35.0±15	10^c	0.83±0.12	120	105	103±18
2.07	$4^+, 1^+$	15.9±5.3	39.0±15	15^c	0.75±0.15	—	123	78±7
2.3-3.1		16.0±5.4	50.0±20	—	—	—	89	113±18
3.1-3.9		13.1±4.4	34.0±14	—	—	150	88	134±15
3.9-4.0		9.6±3.3	11.0±4.5	10^c	0.0 ±0.55	—	114	101±16
0.0-4.0		110. ±36	57.0±22	—	—	81	84	75±8
^{27}Al								
6.7- 7.1		20.3±6.8	55.0±22	—	—	52	75	142±28
7.1- 8.3		19.5±6.5	59.0±24	—	—	183	89	72±20
8.3- 9.2		34.0±10	56.0±23	—	—	59	60	111±26
9.2-10.3		62.0±20	101.0±41	—	—	—	92	90±26
10.3±11.0		66.0±22	64.0±26	—	—	50	61	142±28
11.0-11.4		77.0±25	64.0±26	—	—	—	52	78±14

a — results of analysis using the experimental excitation functions, *b* — results of analysis using the trend free excitation functions, *c* — estimated from the spin values.

of Δ on $C(0)$ can be seen on the right side of Fig. 3. For $\Delta_{\mathrm{cm}} \approx 0.4$ one observes a gradual increase of $C(0)$ with increasing of Δ.

The values of the damping factor D_{eff}, calculated according to A6 (Appendix A) were then used to evaluate the parameter Y_{d} for low states of ^{24}Mg. Necessary values of N_{eff}, listed in Table II, have been calculated using a Hauser-Feshbach formalism (code STATI 2) with optical model parameters taken from Ref. [27] and level density parameters taken from Ref. [28]. For higher multiplets of ^{24}Mg and for all states and multiplets of ^{26}Al the N_{eff} values were estimated by counting the magnetic substates. As can be seen from Tables I and II, when comparing the subcolumns a and b, the procedure of reduction of the experimental data does not produce any bias of the parameters determined. The data in Tables I and II also include the data of summed yields functions of different states. Thus the correlated structures are more pronounced. The purely statistical fluctuations are in this procedure considerably washed up.

The last column of Table II contains the coherence widths Γ_M deduced from the peak counting method [29] using the formula

$$\Gamma_M = \frac{b_n}{2M},$$

where M denotes the number of peaks of $\sigma(E)$ per one MeV in the excitation function and b_n was taken as equal to 0.5. The quoted errors, except Γ_M, listed in Tables II and III are purely statistical ones. The error in Γ_M arises from some uncertainty in the determination of M and b_n. In Table III are given the average coherence widths Γ_a and Γ_M, determined from the experimental and the reduced (trend free) excitation functions for the p, d and α exit channels. The coherence widths, averaged over exit channels and over procedures of determination, are given at the bottom of this Table. A considerable dispersion of Γ, extracted for different channels, indicates the finite range effect of the data used.

A general tendency, which emerges from the inspection of the average values of coherence widths (Table III), is that the values deduced from the trend-free excitation functions are a little smaller than those deduced from the experimental ones. On the average, the Γ_a determined from the trend-free excitation functions is several percent smaller than Γ_M. From Tables II and III we can see that the average values of Γ_a do not change drastically while passing from one channel to another. The average values of Γ_a, for all but the proton groups, are nearly the same. Diminished values of Γ_a, for the proton groups (Table III) reflect the known effect of correlation between Γ_a and $C(0)$ (Γ_a decreases with decreasing $C(0)$ or increasing D_{eff}).

The average coherence width of the ^{28}Si compound nucleus has been determined to be 102 ± 22 keV at the mean excitation of 29.9 MeV. This value is several percent smaller than the coherence width determined in other studies [2, 9, 12, 30] for similar mean values

TABLE III

Average coherence widths

Determined from the trend free excitation functions		Determined from the experimental excitation functions	
Final channel	$\langle\Gamma_a\rangle$ (keV)	$\langle\Gamma_a\rangle$ (keV)	$\langle\Gamma_M\rangle$ (keV)
p	72 ± 17	86 ± 65	106 ± 31
d	111 ± 21	111 ± 29	103 ± 20
α	103 ± 21	123 ± 65	105 ± 24
p, d, α	95 ± 20	107 ± 47	105 ± 24

^{28}Si $\langle\Gamma_c\rangle = (102 \pm 22)$ keV of excitation in ^{28}Si. Examination of the existing data shows that the coherence width remains constant over a large interval of excitation and is independent of the spin and the excitation of the final state. These observations are not consistent with the Hauser-Feshbach calculations made by Gomez del Campo et al. [30], from which it appears that Γ_c depends on the spin and the excitation energy of a final state. From these investigations a rapid growth of Γ_c with increasing excitation energy is expected. On the other hand, Greenwood et al. [9] have shown that at a much higher excitation ($E_{ex} = 39$ MeV) Γ remains practically constant ($\Gamma_c = 112$ keV). However, no calculation performed so far can predict the behaviour of Γ_c in a consistent way.

6. *Evidence for the existence of non statistical phenomena*

The values of Y_d, listed in Tables I and II indicate that a remarkable amount of direct processes is present in the transitions leading to the resolved states, as well as to the groups of unresolved states of all of the residual nuclides. In Fig. 1 vertical lines denote four resonance structures at c.m. energies of 12.57, 12.73, 13.11 and 13.41 MeV, as reported in earlier investigations [11–19]. Besides, a resonance structure is observed also in the region of 13.75 MeV. To see whether these structures really are non statistical we evaluated the deviation function $D(E)$ according to the formula

$$D(E) = \sum_{i=1}^{12} \left(\frac{\sigma_i(E)}{\langle \sigma_i(E) \rangle_I} - 1 \right) \tag{7}$$

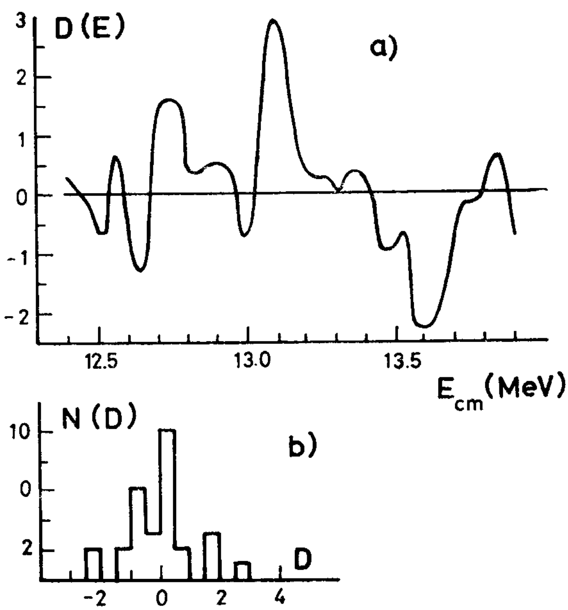

Fig. 6. a) The deviation function $D(E)$ for 12 exit channels of the system $^{12}C + ^{16}O$; b) The probability distribution of the deviations

for the 12 exit channels, those for which the excitation functions are presented in Fig. 1. Results of this evaluation, as shown in Fig. 6a, indicate the existence of correlated structures at energies of ~12.8 and 13.1 MeV, which corresponds to maxima of several excitation functions presented in Fig. 1. The existence of non statistical structures shows up also in the remarkable asymmetry of the distribution of D (Fig. 6b) with respect to $D = 0$. Further evidence for non statistical phenomena will be examined by the cross-correlation analysis and other statistical tests.

7. *Cross-correlation coefficients*

The statistical model predicts that excitation functions for different final channels are uncorrelated. In order to verify this prediction the normalized cross-correlation coefficients $r_{\alpha\beta}$ were calculated for 25 excitation functions according to the formula [31]:

$$r_{\alpha\beta} = \frac{\frac{1}{2}\left[\langle x_\alpha(E)x_\beta(E+\varepsilon)-1\rangle\ \langle x_\alpha(E+\varepsilon)x_\beta(E)-1\right]}{[C_\alpha(\varepsilon)C_\beta(\varepsilon)]^{\frac{1}{2}}}, \tag{8}$$

where α and β denote an arbitrary pair of exit channels, $C_i(\varepsilon)$ is the autocorrelation function for a channel i and

$$x_i(E) = \sigma_i(E)/\langle\sigma_i(E)\rangle.$$

The coefficient $r_{\alpha\beta}$ is equal to ± 1 for the completely correlated transitions and vanishes for the uncorrelated ones. In Fig. 7 are shown histograms of the computed coefficients $r_{\alpha\beta}$ and the statistical distributions calculated from the formula [32]:

$$P_\nu(r) = \frac{\Gamma[(\nu+1)/2]}{\sqrt{\pi}\,\Gamma\left(\frac{\nu}{2}\right)}(1-r^2)^{\frac{\nu-2}{2}}, \tag{9}$$

where $\Gamma(\nu)$ is a gamma function and ν is the number of degrees of freedom. The variable r changes from 0 to 1. The statistical distributions were calculated for $\nu = k-2$, $\nu = \left(\frac{I}{\Gamma_c}-2\right)$ and $\nu = \left(\frac{I}{\pi\Gamma_c}-1\right)$, where k is the number of experimental cross-sections and I is the total energy interval, for which the excitation functions have been measured. This choice of the parameter ν corresponds to the assumptions that cross-sections in channels α and β are: completely uncorrelated, or correlated over the energy interval Γ_c, or correlated over interval $\pi\Gamma_c$, respectively. A broad distribution of the r's deduced from the experimental (non reduced) excitation functions is poorly fitted by any choice of ν (see the right hand side of Fig. 7 for $\varepsilon = 0$). This would suggest that in our case many of the apparent correlations originate from slow energy variation phenomena, which are clearly seen in the proton and, to a smaller degiee, in the deuteron and alpha particle exit channels. The distribution of the r determined for the trend free excitation functions is fairly well fitted by Eq. (9) for $\nu = k-2$. However, small differences between the statistical and actual patterns

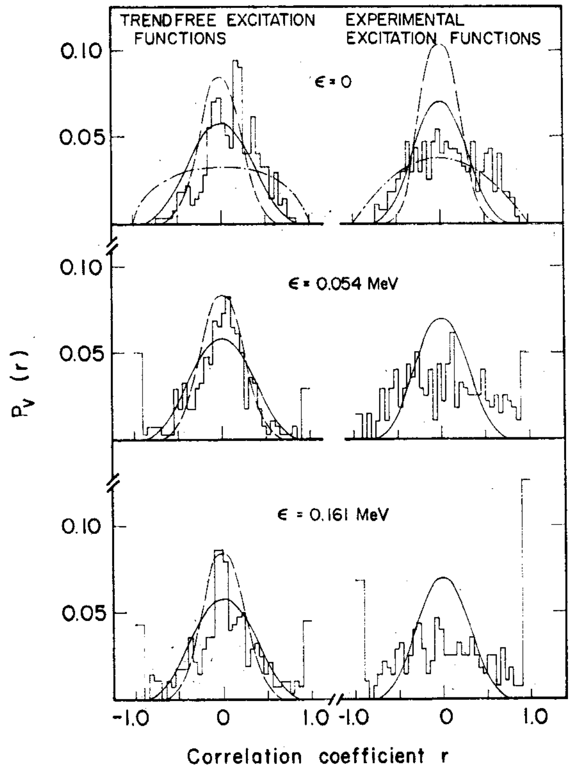

Fig. 7. Distributions of the cross-correlation coefficients r. Histograms correspond to $\Delta = 375$ keV and $\Delta = I$ on the left and right hand side, respectively. The curves calculated with the use of formula (9) correspond to different values of ν: $\left(- - - -\ \nu = k-2,\ \text{———}\ \nu = \frac{I}{\Gamma_c} - 2,\ - \cdot - \cdot -\ \nu = \frac{I}{\pi \Gamma_c} - 2\right)$

show that correlations between different transitions can exist. More pronounced deviations of the cross-correlation distributions from the statistical ones, seen for $\varepsilon > 0$, may be due principally to the finite range of data (FRD) effects. Numerical values of cross--correlation coefficients $r_{\alpha\beta}$ are given in Table IV. Errors of these coefficients listed in Table IV are due to the FRD effects only. The results from Table IV show that transitions to the states of the same nuclide are weakly correlated. The only exceptions are the two pairs of transitions: one to the ground and the 1.37 MeV states and the other to the 5.24 and 6.43 MeV states of ^{24}Mg. In addition, significant correlations exist between the transitions to the ground state and to some closely spaced states forming the multiplets in ^{26}Al. Remarkable correlations are also observed between the channels leading to different multiplets.

In cross-correlation analyses [9, 30] of transitions to higher excited states of ^{24}Mg no remarkable deviations from the statistical mechanism were found. However, Kolata et al. [10] have found in the overlapping region of excitation in the $^{12}C + ^{16}O$ system some significant correlations between the excitation functions for the production of different residual nuclides.

8. Further statistical tests of the resonancelike anomalies

There exist several statistical tests [33, 34] which can be used to show whether experimental data are consistent with the fluctuation pattern or whether they imply the existence in excitation functions of intermediate structures. Two of them, i.e. the distribution of long runs up and down and the distribution of the number of maxima over different excitation functions, were used to detect resonances [33, 35].

The runs up and down are defined as unbroken, linear sequences of increasing or decreasing values of cross-section. For a statistical case the number of runs of a defined length depends only on the sample size. In the region of intermediate structures one can expect that either the length or the number of long runs will be significantly enhanced.

The binomial probability of finding the k accidental maxima in all excitation functions at given incident energy is given by

$$P_W(k, p) = \frac{W!}{k!(W-k!)}(1-p)^{W-k} \cdot p^k, \tag{10}$$

where W is the number of excitation functions corresponding to different reaction channels and p is the average probability for finding a maximum. The probability p was taken to be equal to the ratio of the number of peaks in all excitation functions to the total number of experimental points. All cross-sections fulfilling the condition

$$\sigma(E_{i-1}) < \sigma(E_i) > \sigma(E_{i+1})$$

were regarded as peaks. In Fig. 8 are plotted simultaneously the calculated statistical distributions of the number of peaks and the histogram showing the observed distribution of the

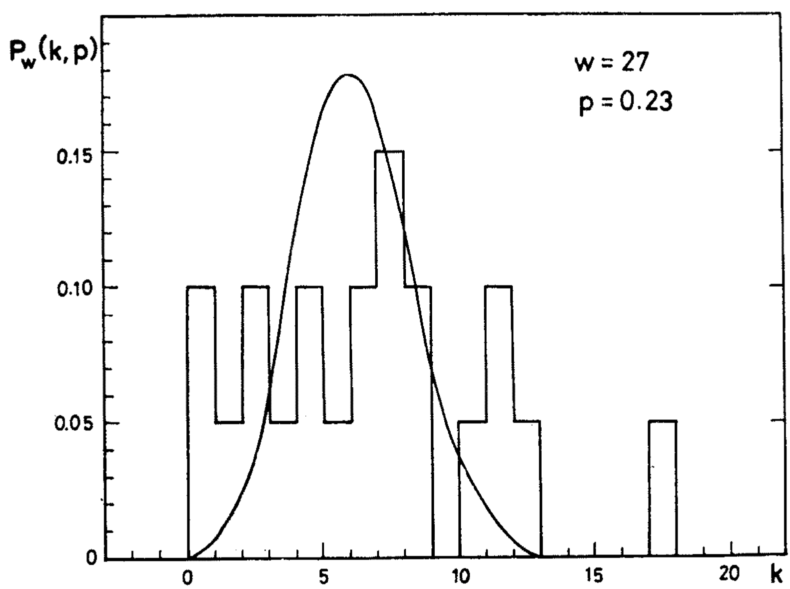

Fig. 8. Histogram and the binomial distribution (according to formula (10)) of the number of maxima at a given energy in different excitation functions

numbers of peaks counted at each energy. An appreciable disagreement between these distributions indicates that the observed structures cannot be of statistical origin.

To make the non statistical structures more visible we have plotted in Fig. 9b the values of k_E multipled by the ratio $P_W(k_M, p)/P_W(k_E, p)$, where k_E is the number of peaks in W excitation functions at a given energy and k_M corresponds to the most abundant number of peaks for pure statistical process. The numerical values of $P_W(k_M, p)$ and $P_W(k_E, p)$ were taken from Fig. 8. The points in Fig. 9b are drawn above the line marking the ratio of probabilities equal to 1 (statistically the most probable case), if $k_E > k_M$ and

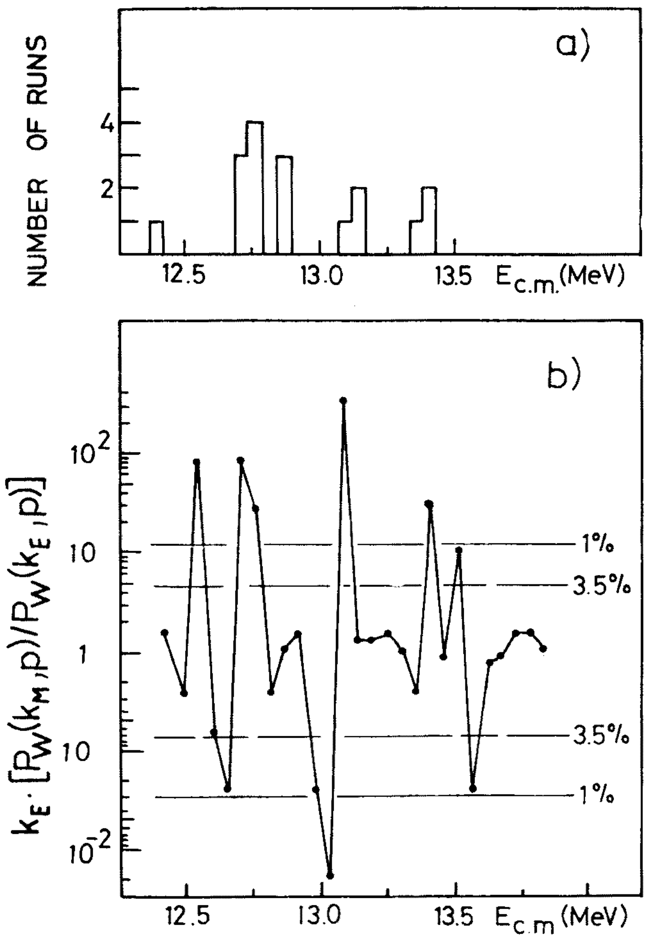

Fig. 9. a) Energy position of long runs with small probability to be of statistical origin; b) The abundance of peaks counted in all excitation functions (at the same energy) and multiplied by the ratio $P_W(k_M, p)/P_W(k_E, p)$ where k_M corresponds to maximum of binomial distribution and k_E is the number of peaks actually observed at energy E. Numerical values of $P_W(k_M, p)$ and $P_W(k_E, p)$ were taken from the calculated distribution presented in Fig. 8. The points were drawn above the value 1 if $k_E > k_M$ and below it if $k_E < k_M$. Significance levels for the statistical process in the amount 1 % and 3.5 % are marked by broken lines

below that line if $k_E < k_M$. Figure 9b also shows the significance levels of 3.5% and 1% as criteria for non statistical phenomena; the number of maxima exceeding the lines 1% or 3.5% is larger than the number of minima.

Distribution of the long runs up and down, shown in Fig. 9a, fits into this pattern. Though this test was considered only a tentative one, it is seen that the runs are clustered around the same energies at which the binomial test detected significant deviations from statistical expectation. Both tests show that non statistical anomalies exist at the energies of 12.57 ± 0.04, 12.73 ± 0.04, 13.11 ± 0.04 and 13.41 ± 0.04 MeV.

The anomaly at 12.57 MeV is distinctly seen in most of the α exit channels as well as in the transitions to the groups of unresolved states in the ^{27}Al nucleus. This anomaly is only marked in the transition to low states of ^{26}Al nucleus and does not appear in the γ-ray yields. A prominent anomaly at 12.73 MeV is observed in all transitions except the ground state of ^{24}Mg and one multiplet of ^{26}Al. At 13.11 MeV there appear prominent peaks in the transition channels to the ground and excited states of ^{24}Mg and ^{26}Al nuclei. The anomalies at 13.41 and 13.51 MeV probably originate from the same structure, the former is seen in the γ, p and α, the later only in the γ and α exit channels. The 7^- resonance at 12.73 MeV is well established. Tentative widths and I^π of resonances found recently [15] in the $^{16}O(^{12}C, {}^{8}Be)$ reaction at energies very close to ours were deduced to be: 420 keV (7^-, 8^+), 500 keV (7^-) and 500 keV (8^+) for the 12.5, 12.8, 13.1 and 13.3 MeV resonances, respectively.

9. *Conclusions*

Although this study was based on the data taken from small sample size, fluctuation analysis of the (^{16}O, p), (^{16}O, d) and (^{16}O, α) reactions on ^{12}C, has been performed for many exit channels. The results indicate that:

1. The coherence widths vary significantly when going from channel to channel.
2. All the statistical tests, explored to distinguish the non statistical structures from that of statistical ones, have consistently lead to locate the presence of non statistical structures at c.m. energies of 12.57, 12.73, 13.11 and 13.41 MeV. Remarkable interchannel correlations were found, as listed in Table IV, mainly between single states and multiplets, as well as between multiplets only. Strong correlations between single states only appear rather in exceptional cases.
3. The contribution of the direct parts of the cross-section, according to the parameter Y_d was found to change considerably in going from channel to channel.

The main conclusion is that through the energy region of $E_{c.m.} = 12.4$–13.9 MeV closely spaced resonances persist. Thus, in this interval of energy there coexist processes which are responsible for the formation of the compound nucleus and simpler intermediate configurations. These results suggest that such an analysis could lead to a discovery of rich resonance pattern in other energy intervals. The energy interval we have examined cannot be exceptional and the excitation of ^{28}Si nucleus under examination was not high enough to terminate the formation of separate resonances.

APPENDIX A

Correction of $C_r(0)$ and Γ_r

The parameters $C_r(0)$ and Γ_c determined from the autocorrelation function $C_r(\varepsilon)$ (formula (2)) are influenced by the experimental conditions i.e. by the counting statistics, the energy resolution and the sample size $n = \frac{I}{\Gamma_c}$, where I is the total energy interval considered. Therefore, these parameters have to be corrected in order to have their true values established. Moreover, the procedure of moving averages causes some reduction of Γ_c. Below are listed some useful phenomenological formulae, based on the results of extensive investigations [2, 8, 22, 23, 25] of synthetic excitation functions. These formulae have been built in such a way that they closely fit the results of Roeders [25] investigations confined within $4 \leqslant \frac{\Delta}{\Gamma_c} \leqslant 15$, where Δ is the energy interval of the moving average. It is believed that they will still be reasonable, if extrapolated to the values of $\frac{\Delta}{\Gamma_c} \approx 3.7$ and $n \leqslant 20$, which is in our case. Under these assumptions the corrected values of $C_n(0)$ and Γ_n can be expressed in the following way:

$$C_n(0) = \alpha_n(\Delta)C_r(0), \qquad \Gamma_n = \beta_n(\Delta)\Gamma_n, \tag{A1}$$

where $C_r(0)$ and Γ_r are the values of the fluctuation parameters extracted from our analysis of the trend-free excitation functions and $\alpha_n(\Delta)$ and $\beta_n(\Delta)$ are correction factors. They were found in such a way as to fit the data of Ref. [25].

$$\alpha_n(\Delta) = \left[1.147+13.644\Big/\left(\frac{\Delta}{\Gamma_c}\right)^2\right]A(n),$$

$$\beta_n(\Delta) = \left[1.073+9.714\Big/\left(\frac{\Delta}{\Gamma_c}\right)^2\right]B(n); \tag{A2}$$

$$A(n) = 0.90+0.005n, \qquad B(n) = 0.83+0.0083n. \tag{A3}$$

Fig. 10 presents the Δ dependence of the correction coefficients α_n and β_n.

After correction of C_n and Γ_n for the finite energy resolution [23] and for the counting statistics [22] one finally gets

$$C(0) = \frac{C_n}{0.62+0.0075n}, \qquad \Gamma_c = \frac{\Gamma_n}{0.68+0.0075n}. \tag{A4}$$

The notation on the left corresponds to that defined in formula (3).

Relative standard deviations (RSD) of $C_n(0)$ and Γ_n, caused by the above mentioned corrections can be estimated according to Dallimore [36] and Roeders [25]:

$$\mathrm{RSD}\,[C_n(0)] = \sqrt{\frac{\pi}{2n}\left(1+\frac{1}{D_{\mathrm{eff}}}\right)},$$

$$\mathrm{RSD}\,[\Gamma_n] = \sqrt{\frac{0.3\pi}{n}\left(1+\frac{1}{D_{\mathrm{eff}}}\right)}, \tag{A5}$$

where D_{eff} is the fluctuation damping factor. For finite sample size it is given by

$$D_{\mathrm{eff}} = \frac{1+a[1+C_n(0)]}{C_n(0)}, \tag{A6}$$

where $a = \frac{2}{n}\,\mathrm{arctg}\,(n) - \frac{1}{n^2}\ln(1+n^2)$. It must be mentioned that the inter- and extra--polations restrict the validity of formulae (A2)–(A4) to $2.5 \leqslant \frac{\Delta}{\Gamma_c} \leqslant 15$ and $5 \leqslant n \leqslant 20$. All the results, on which formulae (A2)–(A4) have been based, were deduced from the synthetic functions with small input parameters N_{eff} and Y_{d}. Because of very weak, if any, dependence of α and β on the N_{eff} and Y_{d} has been observed, it is assumed that these coefficients are independent of the cumulative effect of N_{eff} and Y_{d}, e.g. on D_{eff}.

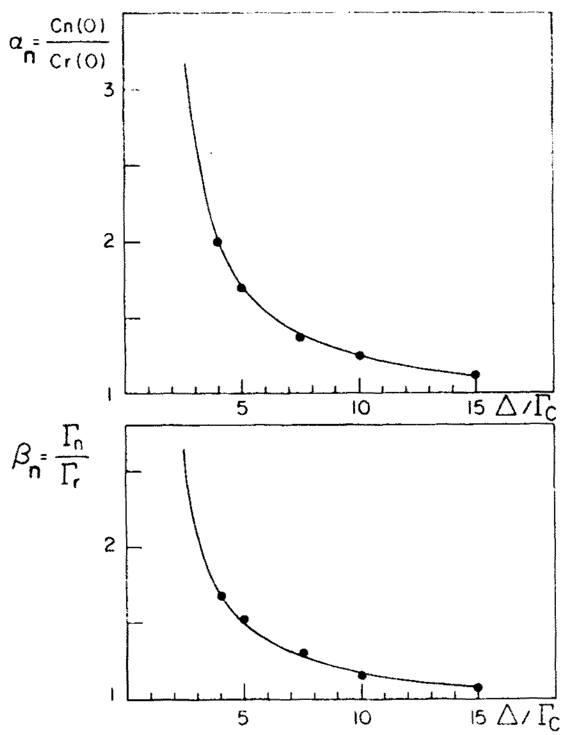

Fig. 10. Dependence of $\alpha_n(\Delta)$ and $\beta_n(\Delta)$ on the width of the averaging interval Δ for fixed sample size of $n = 20$. The full lines represent the fits obtained with the use of formulae (A2) and (A3)

APPENDIX B

Correction of N_r and Y_r

It was shown in Ref. [25] that the formulae (3) and (4) should be conserved if one replaces:

$$N_{\mathrm{eff}} = N_r/\sqrt{\alpha_n},$$

$$Y_{\mathrm{d}} = \{1-\sqrt{\alpha_n}\,[1-(Y_r)^2]\}^{\frac{1}{2}}. \tag{B1}$$

One of the authors, J.S., expresses his gratitude to Prof. P. Taras for hospitality and financial support during his stay at Nuclear Physics Laboratory of Universite de Montreal and for making the experimental results available.

REFERENCES

[1] E. W. Vogt, D. Mc Pherson, J. A. Kuehner, E. Almquist, *Phys. Rev.* **136B**, 84, 99 (1964).
[2] M. L. Halbert, F. E. Durham, A. Van der Woude, *Phys. Rev.* **162**, 899, 919 (1967).
[3] R. G. Stokstad, Int. Conf. on Reactions Between Complex Nuclei, Nashville, North Holland Publishing Comp. 1974, p. 327.
[4] W. Galster, P. Duck, H. Fröhlich, W. Treu, H. Voit, *Nucl. Phys.* **A277**, 126 (1977).
[5] M. Hugi, J. Lang, R. Müller, J. Sromicki, E. Ungricht, K. Bodek, L. Jarczyk, B. Kamys, A. Strzałkowski, H. Witała, *Phys. Rev.* **C25**, 2403 (1982).
[6] W. Hauser, H. Feshbach, *Phys. Rev.* **87**, 366 (1952).
[7] T. Ericson, *Adv. Phys.* **9**, 425 (1960).
[8] T. Ericson, *Ann. Phys.* **23**, 390 (1963).
[9] L. R. Greenwood, K. Katori, R. E. Malmin, T. H. Braid, J. C. Stolzfus, R. H. Siemsen, *Phys. Rev.* **C6**, 2112 (1972).
[10] I. J. Kolata, R. M. Freeman, F. Haas, B. Heusch, A. Gallmann, *Phys. Rev.* **C19**, 408 (1979).
[11] J. R. Patterson, B. N. Nagorcka, G. D. Symons, W. M. Zuk, *Nucl. Phys.* **A165**, 545 (1971).
[12] R. E. Malmin, J. W. Harris, P. Paul, *Phys. Rev.* **C18**, 163 (1978).
[13] P. Taras, G. R. Rao, *Phys. Rev.* **C19**, 1557 (1979).
[14] P. Taras, G. R. Rao, G. Azuelos, *Phys. Rev. Lett.* **41**, 840 (1978).
[15] J. R. Hurd, N. R. Fletcher, A. D. Frawley, J. F. Mateja, *Phys. Rev.* **C22**, 528 (1980).
[16] A. D. Frawley, N. R. Fletcher, L. C. Dennis, *Phys. Rev.* **C25**, 860 (1982).
[17] Z. E. Switkowski, H. Winkler, P. R. Christensen, *Phys. Rev.* **C15**, 449 (1977).
[18] F. Soga, J. Schimizu, H. Kamitsubo, N. Takahashi, K. Takimoto, R. Wada, T. Fujisawa, T. Wada, *Phys. Rev.* **C18**, 2457 (1978).
[19] D. Branford, J. O. Newton, J. M. Robinson, B. N. Nagorcka, *J. Phys. A* **7**, 1193 (1974).
[20] G. Pappalardo, *Phys. Lett.* **13**, 320 (1964).
[21] T. Ericson, T. Mayer-Kuckuk, *Ann. Rev. Nucl. Sci.* **16**, 183 (1966).
[22] L. W. Put, J. D. A. Roeders, Van der Woude, *Nucl. Phys.* **A112**, 561 (1968).
[23] A. Van der Woude, *Nucl. Phys.* **80**, 14 (1966).
[24] D. Shapira, R. G. Stokstad, D. A. Bromley, *Phys. Rev.* **C10**, 1063 (1974).
[25] J. D. A. Roeders, *Intern. Rapport* I.V.I. 23 (1971).
[26] H. Witała, L. Jarczyk, A. Strzałkowski, J. Lang, R. Müller, *Acta Phys. Pol.* **B14**, 555 (1983).
[27] *Atomic Data and Nuclear Data Tables*, vol. **17**, No 1 (1976).
[28] A. Gilbert, A. G. W. Cameron, *Can. J. Phys.* **43**, 1446 (1965).
[29] P. G. Bizetti, P. R. Maurenzig, *Nuovo Cimento* **47B**, 29 (1967).

[30] J. Gomez del Campo, M. E. Ortiz, A. Dacal, J. L. C. Ford, L. R. Robinson, P. H. Stelson, *Nucl. Phys.* **A262**, 125 (1976).
[31] J. Barrette, M. J. LeVine, P. Braun-Munzinger, G. M. Berkowitz, M. Gai, J. W. Harris, C. M. Jachcinski, C. D. Uhlhorn, *Phys. Rev.* **C20**, 1759 (1979).
[32] P. R. Bevington, *Data Reduction and Error Analysis for the Physical Sciences*, Mc Graw-Hill, Inc. 1969.
[33] Y. Baudinet-Robinet, C. Mahaux, *Phys. Rev.* **C9**, 723 (1974).
[34] L. C. Dennis, S. T. Thornton, K. R. Cordell, *Phys. Rev.* **C19**, 777 (1979).
[35] Y. Baudinet-Robinet, C. Mahaux, *Phys. Lett.* **42B**, 392 (1972).
[36] P. J. Dallimore, I. Hall, *Nucl. Phys.* **88**, 193 (1966).

TABLE IV

Cross – correlation coefficients r

		^{24}Mg										^{26}Al									^{27}Al					
	Ex, J^{π}	0, 0^+	1.37, 2^+	4.12, 4^+ 4.23, 2^+	5.24, 3^+	6.01, 4^+	6.43, 0^+	0-6.43	7.1-8.0	8.0-8.4	7.1-10.0	0, 5^+	0.42, 3^+	1.06, 1^+	1.76, 2^+ 1.85, 1^+	2.07, 4^+ 2.072, 1^+	2.3-3.1	3.1-3.9	3.9-4.0	0-4.0	6.4-7.1	7.1-8.3	8.3-9.2	9.2-10.3	10.3-11.0	11.0-11.4
^{24}Mg	0, 0^+		-0.66 ±0.16							0.29 ±0.15					-0.29 ±0.13						-0.37 ±0.09		0.25 ±0.07	-0.38 ±0.05	0.36 ±0.05	
	1.37, 2^+			0.36 ±0.06							-0.36 ±0.04	-0.37 ±0.09					0.42 ±0.04		-0.32 ±0.06		0.27 ±0.04		-0.39 ±0.03		0.47 ±0.03	
	4.12, 4^+ 4.23, 2^+				0.33 ±0.09		0.46 ±0.1			0.37 ±0.06	-0.50 ±0.03					0.45 ±0.05	0.62 ±0.04		-0.49 ±0.05	-0.53 ±0.05	0.31 ±0.04				0.35 ±0.03	
	5.24, 3^+					0.41 ±0.09	0.71 ±0.14				0.33 ±0.05	0.51 ±0.13				0.27 ±0.08	0.72 ±0.07	-0.32 ±0.08	0.36 ±0.08	0.43 ±0.04		0.29 ±0.06			0.55 ±0.04	-0.26 ±0.04
	6.01, 4^+											0.36 ±0.09			0.60 ±0.06	0.41 ±0.05	0.34 ±0.04		0.36 ±0.06	0.39 ±0.06	-0.43 ±0.04	0.31 ±0.04				
	6.43, 0^+											0.39 ±0.14			0.25 ±0.09		0.69 ±0.07			0.36 ±0.04			0.43 ±0.05	0.45 ±0.04	0.67 ±0.04	
	0-6.43								0.37 ±0.04								0.62 ±0.04	0.27 ±0.05							0.43 ±0.02	
	7.1-8.0									-0.50 ±0.04		0.50 ±0.06			-0.30 ±0.04	0.54 ±0.03			0.54 ±0.04	0.52 ±0.02		0.40 ±0.03				
	8.0-8.4											-0.42 ±0.09				0.54 ±0.05			0.44 ±0.06	-0.43 ±0.03		-0.40 ±0.04				0.37 ±0.03
	7.1-10.0											0.69 ±0.04	0.32 ±0.03			0.75 ±0.03			0.94 ±0.03	0.88 ±0.02	-0.31 ±0.02	0.42 ±0.02		0.32 ±0.02		
^{26}Al	0, 5^+												0.30 ±0.06		0.36 ±0.08	-0.75 ±0.07		0.25 ±0.07	0.82 ±0.08			0.81 ±0.05	0.48 ±0.04	0.60 ±0.04	0.55 ±0.04	
	0.42, 3^+													0.61 ±0.05	0.25 ±0.04			0.35 ±0.04	0.34 ±0.04				0.28 ±0.02	0.25 ±0.02	0.29 ±0.02	0.60 ±0.02
	1.06, 1^+														0.26 ±0.07	-0.53 ±0.06		0.48 ±0.06					0.25 ±0.04			0.64 ±0.03
	1.76, 2^+ 1.85, 1^+															0.32 ±0.05	0.30 ±0.04		0.34 ±0.05			0.43 ±0.04		0.61 ±0.03	0.27 ±0.03	0.62 ±0.03
	2.07, 4^+ 2.072, 1^+																		0.91 ±0.05			0.75 ±0.03		0.48 ±0.02		
	2.3-3.1																								0.27 ±0.02	
	3.1-3.9																					-0.47 ±0.03				0.39 ±0.02
	3.9-4.0																					0.62 ±0.04		0.49 ±0.02	0.25 ±0.02	
	0-4.0																				-0.25 ±0.02	0.41 ±0.02		0.51 ±0.01		
^{27}Al	6.4-7.1																					0.36 ±0.03	0.46 ±0.02	0.51 ±0.02		
	7.1-8.3																						0.50 ±0.02	0.64 ±0.02	0.46 ±0.02	
	8.3-9.2																							0.43 ±0.02	0.77 ±0.01	0.39 ±0.02
	9.2-10.3																								0.38 ±0.01	0.53 ±0.01
	10.3-11.0																									0.33 ±0.01